

1987

Importance of Space-Charge Effects in Resonant Tunneling Devices

M. Cahay
Purdue University

M. McLennan
Purdue University

D. Datta
Purdue University

Mark S. Lundstrom
Purdue University, lundstro@purdue.edu

Follow this and additional works at: <https://docs.lib.purdue.edu/ecepubs>

 Part of the [Electrical and Computer Engineering Commons](#)

Cahay, M.; McLennan, M.; Datta, D.; and Lundstrom, Mark S., "Importance of Space-Charge Effects in Resonant Tunneling Devices" (1987). *Department of Electrical and Computer Engineering Faculty Publications*. Paper 79.
<http://dx.doi.org/10.1063/1.98097>

This document has been made available through Purdue e-Pubs, a service of the Purdue University Libraries. Please contact epubs@purdue.edu for additional information.

Importance of space-charge effects in resonant tunneling devices

M. Cahay, M. McLennan, S. Datta, and M. S. Lundstrom

Citation: **50**, 612 (1987); doi: 10.1063/1.98097

View online: <http://dx.doi.org/10.1063/1.98097>

View Table of Contents: <http://aip.scitation.org/toc/apl/50/10>

Published by the [American Institute of Physics](#)

Importance of space-charge effects in resonant tunneling devices

M. Cahay, M. McLennan, S. Datta, and M. S. Lundstrom

School of Electrical Engineering, Purdue University, West Lafayette, Indiana 47907

(Received 5 November 1986; accepted for publication 6 January 1987)

The consideration of space charge in the analysis of resonant tunneling devices leads to a substantial modification of the current-voltage relationship. The region of negative differential resistance (NDR) is shifted to a higher voltage, and broadened along the voltage axis. Moreover, the peak value of current prior to NDR is reduced, leading to a reduction in the predicted peak-to-valley ratio. An approach is presented to include space-charge effects, and a recently fabricated GaAs-Al_xGa_{1-x}As structure is analyzed, to underscore the importance of a self-consistent electrostatic potential in theoretical calculations.

Since the pioneering work of Tsu and Esaki,^{1,2} there has been a growing interest in double-barrier resonant tunneling devices. Structures grown by both molecular beam epitaxy (MBE)³ and metalorganic chemical vapor deposition (MOCVD)⁴ have been reported with improving peak-to-valley ratios, exhibiting negative differential resistance (NDR) at room temperature. It has often been suggested³⁻⁷ that the presence of electrons could substantially affect the shape of the electrostatic potential in the devices, since the well acts as a dynamic trap for the tunneling electrons. Some authors have estimated that modifications of 10 meV or 0.1 eV could occur in the conduction-band energy profile.^{5,6} Very recently, a quantitative calculation illustrating the effect of space charge on the current-voltage (*I-V*) characteristic has been reported.⁸ However, as discussed later, our results are significantly different; this is possibly because of two assumptions made in Ref. 8 that are different from our model. In this letter, we investigate the space-charge effects in resonant tunneling devices and perform a fully self-consistent calculation of an *I-V* characteristic. We compare our results to the usual approach, in which space-charge effects are completely neglected, and the application of an external bias is assumed to result in a linear voltage drop across the device. Hereafter, the latter approach will be referred to as "flatband theory."

In equilibrium, the inclusion of self-consistency is achieved as follows. The conduction-band profile is initially assumed to be the "flatband" profile, including only the variations due to band-gap discontinuities for the differing materials. Electron density can be calculated by solving the Schrödinger equation; this result modifies the net charge density in the device, and in turn, leads to a new solution for electrostatic potential from the Poisson equation. The calculations for electron density and electrostatic potential are performed iteratively, until the electrostatic potential converges to a final solution. For structure under bias, a linear voltage drop applied to the equilibrium solution serves as an initial guess, and iteration is continued until self-consistency is established. The fully self-consistent potential is then used to calculate current density.

Following Vassell *et al.*,⁷ we calculate the electronic current of a device by solving the Schrödinger equation, with the usual boundary conditions for plane-wave solutions.¹ The effective-mass variation across the device is included by requiring everywhere the continuity of the wave function, and

its first derivative divided by the electron effective mass. The transmission coefficient *T* is then obtained using the transfer-matrix technique,^{2,7} from which the current density can be deduced using

$$J = \frac{em_c^*}{2\pi^2\hbar^2} \int_0^\infty dE_t \int_0^\infty dE_l T(E_l, E_t) [f(E) - f(E + eV)], \quad (1)$$

where *E_l* and *E_t* are, respectively, the longitudinal and transverse component of the electron total energy *E*; *f*(*E*) is the Fermi-Dirac distribution function; *V* is the bias applied across the structure; and *m_c^{*}* is the electron effective mass in the contact. This is the same formula used in the flatband theory; however, we perform the calculation of electrostatic potential, and hence the transmission coefficient, self-consistently. To save computation time, we follow Vassell *et al.*⁷ and assume that the transverse energy *E_t* is equal to its thermal average, *k_BT*. Hence, the transmission coefficient becomes a function of longitudinal energy only, and the integration over transverse energy can be performed analytically. This same assumption also applies in the derivation of electron density.

The electron density is calculated by considering two streams of electrons impinging from the contacts. For electrons incident from the left, we have a density given by

$$n^{l-r}(z) = \int_0^{+\infty} \frac{dk_z}{2\pi} |\psi_{k_z}^{l-r}(z)|^2 \sigma^{l-r}(k_z), \quad (2)$$

where

$$\sigma^{l-r}(k_z) = \frac{m_c^* k_B T}{\pi \hbar^2} \ln \left[1 + \exp \left(\frac{E_l - E_C(0) - \hbar^2 k_z^2 / 2m_c^*}{k_B T} \right) \right], \quad (3)$$

E_C(0) being the bottom of the conduction band in the left contact, which is hereafter taken as a reference point, i.e., *E_C*(0) = 0. Following a similar derivation, the charge density associated with electrons impinging from the right is given by an expression similar to Eq. (2); however, the wave function must be calculated for the opposite flow of electrons, and the factor *σ*(*k_z*) must be referenced to the conduction-band edge in the right contact, *E_C*(*L*).

The modification of the electrostatic potential due to the electron density is then calculated by solving the Poisson equation between the two contacts:

$$\frac{d}{dz}\left(\epsilon(z)\frac{d}{dz}\Phi(z)\right) = -q[N_D^+(z) - N_A^-(z) - n(z)], \quad (4)$$

allowing for a position-dependent dielectric constant $\epsilon(z)$. In Eq. (4), $\Phi(z)$ is the electrostatic potential, and N_A^- , N_D^+ are the ionized acceptor and donor impurity concentrations throughout the device. As many as 15 iterations are sometimes required between Eqs. (2) and (4) to obtain current densities with three significant figures.⁹

Figure 1(a) shows the cross section of a resonant tunneling device fabricated by Ray *et al.*,⁴ which we have chosen to examine. The structure is typical of those proposed or fabricated, with heavily doped contacts ($2 \times 10^{18} \text{ cm}^{-3}$) for a large resonant tunneling current, and undoped "spacer" layers on either side of the double barrier region. The inclusion of spacer layers has several advantages. First, the spacer layers tend to reduce the migration of impurities from the contact regions to the resonant tunneling region, thereby reducing impurity scattering in the barrier and well regions. Second, a greater degree of symmetry in the conduction-band energy profile is maintained, since an applied bias is dropped across a longer, undoped region. As Ricco and Azbel pointed out,¹⁰ asymmetry in the conduction-band profile degrades the peak in resonant transmission, reducing the resonant tunneling effect. Finally, the presence of spacer layers pronounces the upward shift of the conduction-band profile in the undoped region, reducing the component of ther-

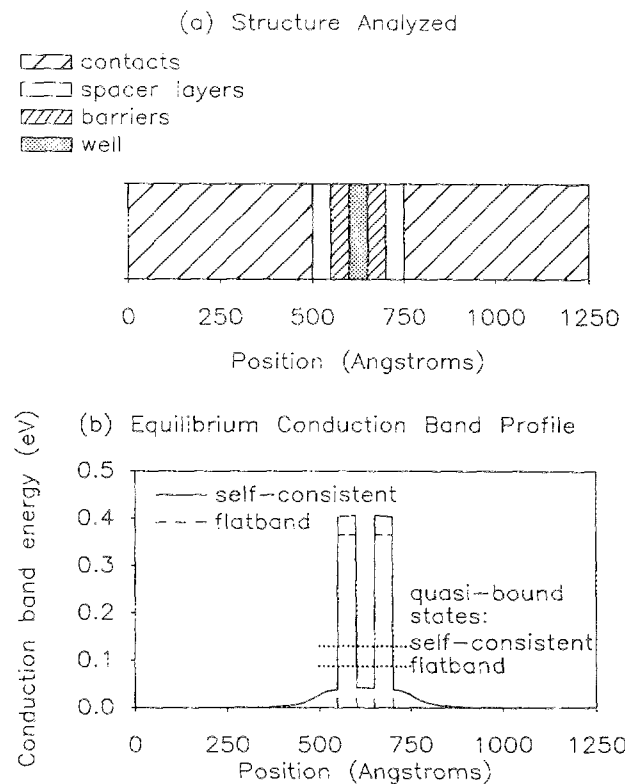


FIG. 1. (a) Structure fabricated by Ray *et al.* (Ref. 4). Contact regions are GaAs doped $2 \times 10^{18} \text{ cm}^{-3}$ (Te); spacer regions are undoped GaAs; barriers are undoped $\text{Al}_{0.45}\text{Ga}_{0.55}\text{As}$; and the well is undoped GaAs. (b) Equilibrium conduction-band profiles for self-consistent and flatband calculations.

mionic emission current over the top of the barriers. This upward shift is explicitly taken into account in our self-consistent calculations, and is illustrated for the equilibrium case in Fig. 1(b).

The current-voltage characteristics calculated for the structure of Fig. 1(a) are presented in Fig. 2, showing both self-consistent and flatband results. Note that the position of NDR is higher along the voltage axis for the self-consistent case. The consideration of space-charge shifts the conduction-band edge upward in the undoped region, pushing the quasi-bound state in the well farther from the conduction-band edge in either contact [see Fig. 1(b)]. Since the voltage at which NDR is observed depends on this distance, an upward shift of the quasi-bound state causes a translation of NDR along the voltage axis. Moreover, the magnitude of this translation will be approximately twice that of the quasi-bound state shift, since it requires a bias of approximately twice the height of the quasi-bound state above the conduction-band edge in the contact to observe NDR. For the structure of Fig. 1, the upward shift of the quasi-bound state due to the consideration of space charge is approximately 0.042 eV, leading to a translation in the NDR region of nearly 0.1 V, relative to flatband calculations.

Returning to Fig. 2, we note that the inclusion of self-consistency has broadened the NDR region. In the self-consistent calculation, current density reaches a maximum when the quasi-bound state level is well above the conduction-band edge in the contact. This is illustrated in Fig. 3, which presents plots of the conduction-band profile at biases corresponding to current maxima (points P and Q of Fig. 2) for (a) flatband and (b) self-consistent calculations. After the maximum current is attained, therefore, a larger additional bias is required in the self-consistent case to pull the resonant level below the conduction-band edge in the contact, and reach the point of minimum current. The result is a broadening of the self-consistent NDR region, compared to the flatband solution.

Finally, the peak current of the NDR region is reduced

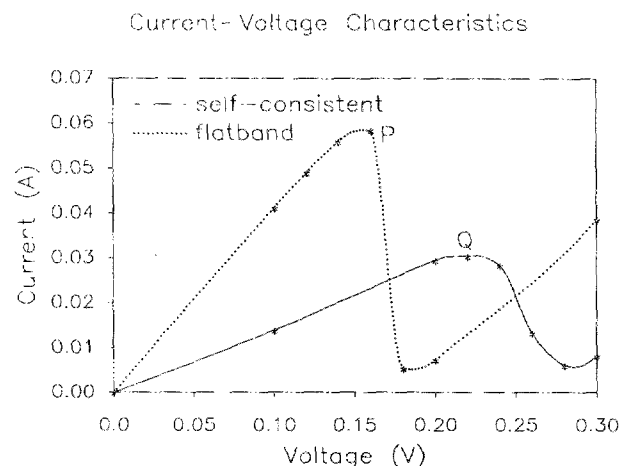


FIG. 2. Current-voltage characteristics (both self-consistent and flatband results) for the structure of Fig. 1, at 300 K. Note that the inclusion of self-consistency has shifted the position of NDR to a higher bias, and broadened the characteristic. In addition, the peak current is reduced for the self-consistent calculation.

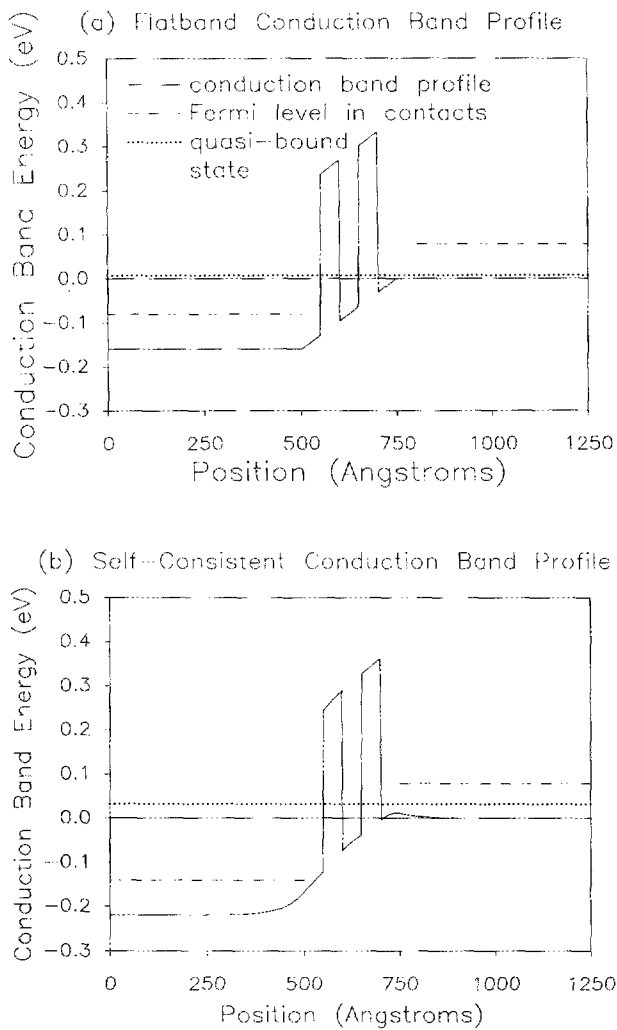


FIG. 3. Conduction-band profile for biases of current maxima, for (a) flatband analysis (point *P* of Fig. 2) and (b) self-consistent analysis (point *Q* of Fig. 2). The level of the quasi-bound state is well above the conduction-band edge in the contact, for the self-consistent case.

for the self-consistent calculation. Since the onset of NDR occurs at a higher bias in the self-consistent case, the transmission coefficient is severely degraded. Current is maximized when the product of a degrading transmission peak and an increasing flux of incident electrons is maximized. As mentioned above, this occurs when the quasi-bound state energy is well above the conduction-band edge in the contact. For the structure of Fig. 1, the valley currents in both self-consistent and flatband analyses are nearly equal. The reduction in peak current, therefore, leads to an overall re-

duction in the peak-to-valley ratio for the self-consistent result. For the flatband analysis, the peak-to-valley ratio is 10.6:1, this is reduced to 4.95:1 for self-consistent calculations.

Similar calculations have been published quite recently,⁸ leading to similar conclusions. However, there are two assumptions made in Ref. 8 that are different from ours. First, the electron density is calculated quantum mechanically only in the quantum well and the barriers; outside the barriers, such as in the buffer regions and in the contacts, the electron density is calculated classically. In our calculations, the electron density is calculated quantum mechanically everywhere in the device. Second, in Ref. 8 the transverse energy E_t of the electrons is assumed to be zero while we replace E_t by its thermal average $k_B T$. On applying our technique to the device considered in Ref. 8, we find a peak current density lower by a factor of 3. Furthermore, the upward shift in voltage of the self-consistent NDR region, compared to the flatband result, is reduced by a factor of 4. This highlights the sensitivity of I - V calculations, with respect to space-charge effects.

Although the inclusion of self-consistency improves agreement between theory and experiment, meaningful comparison must await a more precise knowledge of device parameters (e.g. doping densities, interface and bulk charges, contact resistances, etc.), and a realistic treatment of carrier scattering. It has recently been suggested that sequential tunneling, rather than coherent resonant tunneling, is the relevant mechanism for the operation of quantum-well diodes.¹¹ However, an analysis of this effect requires a proper treatment of carrier scattering within the device, and remains a goal of future research. Nevertheless, the conclusions of this work emphasize the importance of space-charge effects in the analysis of resonant tunneling devices.

This work was supported by the Semiconductor Research Corporation under contract 86-07-089.

¹L. Esaki and R. Tsu, *IBM J. Res. Dev.* **14**, 61 (1970).

²R. Tsu and L. Esaki, *Appl. Phys. Lett.* **22**, 562 (1973).

³T. J. Shewchuk, P. C. Chapin, P. D. Coleman, W. Kopp, R. Fisher, and H. Morkoç, *Appl. Phys. Lett.* **46**, 508 (1985).

⁴S. Ray, P. Ruden, V. Sokolov, R. Kolbas, T. Boonstra, and J. Williams, *Appl. Phys. Lett.* **48**, 1666 (1986).

⁵B. Jogai, K. L. Wang, and K. W. Brown, *J. Appl. Phys.* **59**, 2968 (1986).

⁶J. N. Schulman, *Appl. Phys. Lett.* **49**, 690 (1986).

⁷M. O. Vassell, Johnson Lee, and H. F. Lockwood, *J. Appl. Phys.* **54**, 5206 (1983).

⁸H. Ohnishi, T. Inata, S. Muto, N. Yokoyama, and A. Shibatomi, *Appl. Phys. Lett.* **49**, 1248 (1986).

⁹Detailed results will be published elsewhere.

¹⁰B. Ricco and M. Ya. Azbel, *Phys. Rev. B* **29**, 1970 (1984).

¹¹S. Luryi, *Appl. Phys. Lett.* **47**, 490 (1985).